SUPPORT VECTOR MACHINE (SVM) ACTIVE LEARNING FOR AUTOMATED GLIOBLASTOMA SEGMENTATION

Po Su[1,3], Zhong Xue[1], Linda Chi[2], Jianhua Yang[3], Stephen T. Wong[1,2]*

[1]Department of Systems Medicine and Bioengineering, The Methodist Hospital Research Institute, Weill Cornell Medical College, Houston, TX; [2]Department of Diagnostic Radiology, MD Anderson Cancer Center, Houston, TX; [3]School of Automation, Northwestern Polytechnical University, China
E-mail: zxue@tmhs.org

ABSTRACT

Accurate segmentation of Glioblastoma multiforme (GBM) from MR images is important for sub-typing in diagnosis, determining tumor margins in surgical planning, and selecting appropriate therapies. However, it is a challenging and time-consuming task because GBM has a variety of imaging characteristics and often deforms nearby tissues in the brain. In this paper, we propose a support vector machine (SVM) active learning approach to address the problem of GBM segmentation from multi-modal MR images. First, a knowledge–based fuzzy clustering algorithm is performed to segment the brain tissues into six classes including white matter (WM), grey matter (GM), cerebrospinal fluid (CSF), T2-hyperintense regions, necrosis and enhanced tumor. Then, the SVM active learning approach is applied to refine the segmentation. Comparative studies with other segmentation methods indicate that the proposed algorithm can segment GBM more accurately.

Index Terms— Glioblastoma, clustering, SVM, active learning

1. INTRODUCTION

Glioblastoma multiforme (GBM) is the most common and aggressive malignant brain tumor in human, which accounts for 40% of brain tumors and has very short postoperative survival time (the median is 14 months) [1, 2]. Generally, in contrast enhanced MR images, GBM consists of enhancing tumor, necrosis, and non-enhancing tumor, including edema. The enhancement of the tumor is related to integrity of the blood-brain-barrier and angiogenesis. In multimodal MR (T1- and T2-weighted, T1 post-contrast, and FLAIR images) images, these three parts of GBM can be visually assessed. Enhanced tumor can be clearly seen from T1 post-contrast images but non-enhanced tumor often overlaps with edema by visual assessment. Quantitative segmentation is thus important to segment GBM in detail and to help neuroradiologists determine the tumor margin. Therefore, our goal is to quantify GBM using multimodal MR images, which, combined together, provide sufficient tissue information. Typically, T1 post-contrast MRI shows enhanced tumor well, and the entire tumor region demonstrates lower intensity in T1-weighted images. T2-weighted and FLAIR MRI are useful to highlight all the three parts in different intensity levels, and non-enhanced tumor also shows up with slightly lower T2 and FLAIR intensities.

To date, the detailed marginal analysis and judgment of the tumor aggressiveness are dependent on the experience of neuroradiologists. In order to facilitate the GBM aggressiveness diagnosis and determine tumor margins, in this paper, we propose a detailed GBM quantification method. Moreover, recently, TCGA researchers have established the existence of four subtypes of GBM defined by genomic characteristics. This is an important first step towards developing personalized treatments that target the unique genetic alteration in each subtype [3]. Quantification of GBM from MR images could potentially correlate with the TCGA sub-typing and provide important neuroradiology clinical criteria for GBM diagnosis and treatment.

In addition to deformable model-based shape matching [4], the unsupervised clustering methods are popular. For example, Clark et al. [5] developed a knowledge-based fuzzy clustering algorithm to segment GBM. The initial segmentation is performed using fuzzy C-mean clustering algorithm. The result is then refined based on the knowledge of cluster distribution and anatomical information. However, clustering methods often suffer from overlapping intensity distributions of different tissues. Thus, it is essential to combine other information to improve the results. Some supervised classifiers were investigated [6-8] but they require a lot of manually segmented data to train the model. Corso et al. [9] integrated the Bayesian model classification with graph-based affinities to segment brain tumor in multimodal MR images. Prastawa et al. [10] considers tumor as outliers of normal voxel distribution, so that tumor and edema are isolated by a statistical classification based on learning voxel-intensity distributions for normal brain tissues.

In fact, a properly designed training sample sets can improve the segmentation results. In this paper, we proposed

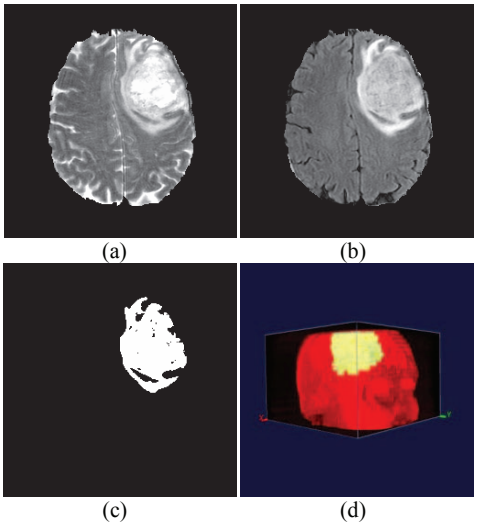
a SVM active learning approach to GBM segmentation using multimodal MR brain images. Based on the initial segmentation using knowledge-based fuzzy clustering algorithm [5], the active learning algorithm is incorporated with SVM to select the training samples that can best represent each class and perform the classification iteratively. In our studies, the SVM active learning approach is validated using multimodal MR images, and the segmentation results showed the superiority of our algorithm. Finally, as an application, we demonstrate that the joint intensity color-map on the edema region might give detailed transition area from enhanced tumor to the edema, which can help determine the tumor margin of GBM.

2. METHOD

The proposed method consists of two main steps. The first step is initial segmentation of GBM using knowledge-based fuzzy clustering algorithm [5], and the second step is the proposed SVM active learning method to optimize the training set and refine the segmentation.

2.1. Initial Segmentation of GBM Using Knowledge-Based FCM

The preprocessing steps include co-registration of the multimodal images and skull stripping. For co-registration, T2, FLAIR and T1 pre-contrast images of each subject are registered onto the T1 post-contrast image using a rigid registration with mutual information [11]. For skull stripping, a manual skull stripped template is registered onto each subject's T1 post-contrast image and then used as a brain mask to eliminate the skulls [12].

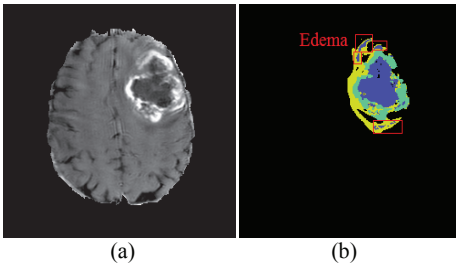


(a) (b) (c) (d)

Fig 1. Segmentation of abnormal region. (a) T2; (b) FLAIR; (c) abnormal region extraction; (d) 3D rendering.

After preprocessing, the knowledge-based fuzzy clustering algorithm [5] is used for initial brain tissue segmentation. This brain tissue segmentation consists of two steps. First, the normal tissues (WM, GM, and CSF) and abnormal regions are segmented using $\{I_{T2}, I_{FLAIR}\}$ as the feature sets because the abnormal regions have high intensity in T2 and FLAIR. Fig. 1 shows an example of the input images and the segmented results.

Then the abnormal area including edema, necrosis, and enhanced tumor are segmented by performing FCM again with $\{I_{T2}, I_{T1PRE}, I_{T1POST}\}$ as the features, because T1 has good discrimination on necrosis and enhanced tumor, and T2 contains more edema information. Fig. 2 shows the result of GBM tissue segmentation.



(a) (b)

Fig 2. Segmentation of enhanced tumor, necrosis, and edema. (a) T1 post-contrast; (b) segmentation result.

2.2. SVM Active Learning Algorithm

Notice that in the above segmentation there are still some tissue overlapping as shown in Fig. 2 (b), where some edema might be segmented as necrosis. The proposed SVM active learning approach is then applied to refine the results, $\{I_{T2}, I_{T1PRE}, I_{T1POST}, I_{FLAIR}\}$ are utilized as the feature set.

2.2.1. Support Vector Machine

SVM has been recognized as a powerful tool with state-of-the-art performance on classification. The basic idea of SVM is mapping the inputs to a high-dimensional feature space and finding a separating hyper plane with maximal margin between the two classes by optimizing the classification function:

$$f(x) = \sum_{i=1}^{m} \alpha_i y_i \langle \varphi(\mathrm{x}_i), \varphi(\mathrm{x}) \rangle + b = \sum_{i=1}^{m} \alpha_i y_i K(\mathrm{x}_i, \mathrm{x}) + b\,, \quad (1)$$

where $\mathrm{x}_i \in R^n$ is a vector containing n attributes of voxel i, and $y_i \in \{+1, -1\}$ is the class label of the voxel. $K(\mathrm{x}_i, \mathrm{x}_j) = \langle \varphi(\mathrm{x}_i), \varphi(\mathrm{x}_j) \rangle$ is the kernel function of the nonlinear mapping φ. In the high-dimensional space defined by φ, the separating hyper plane is a linear combination of $\varphi(\mathrm{x}_i)$.

$$\mathrm{w} = \sum_{i=1}^{m} \alpha_i y_i \, \varphi(\mathrm{x}_i). \quad (2)$$

In case such separating hyper plane does not exist, a slack variable ξ_i is introduced, such that

$$y_i[(\mathrm{w} \cdot \mathrm{x}_i) + b] \geq 1 - \xi_i\,, \quad \xi_i > 0, \quad (3)$$

and the optimizing classification function becomes,

$$Mininize \qquad \frac{1}{2}\|\mathrm{w}\|^2 + C\sum_{i=1}^{m}\xi_i$$
$$s.t. \qquad y_i[(\mathrm{w}\cdot \mathrm{x}_i)+b] \geq 1-\xi_i\,, \quad \xi_i > 0. \qquad (4)$$

By solving the quadratic programming optimization problem, the optimal values of α is obtained and the decision function is:

$$f(x) = sign\left(\sum_{i=1}^{m}\alpha_i y_i K(\mathrm{x}_i,\mathrm{x}) + b\right). \qquad (5)$$

The binary classification SVM can be extended to multi-classification using one-against-all or one-against-one method [13]. In this work the one-against-one strategy is adopted.

2.2.2. SVM Active Learning

For supervised learning, it is crucial to select the most valuable training data for better performance. In GBM segmentation, the training data of one tissue type generated from first step often contain unwanted samples from other tissue type. In order to achieve accurate segmentation, we propose to combine the idea of active learning [14] with SVM for refinement of GBM segmentation.

List 1. SVM active learning algorithm

1. Apply the C-step operation to select the training data sets from each class (see List. 2).
2. Train the SVM and classify all the voxels into six classes, i.e., enhanced tumor, edema, necrosis, WM, GM and CSF.
3. Compute the mean $\bar{X}_l^{\,j}$ of each class. $l = 1,2\cdots 6$ indicate the class index, j indicates the iteration number.
4. Set $j=j+1$, and repeat (1)(2)(3), until

$$\max_i \left\| \bar{X}_l^{\,j+1} - \bar{X}_l^{\,j} \right\| \leq \varepsilon \qquad (6)$$

List 2. C-step operation

1. Given the current segmentation results, compute the mean $\bar{X}_l = (\overline{x_{l1}}, \overline{x_{l2}}, \overline{x_{l3}}, \overline{x_{l4}})^T$ as the estimated center of this class.
2. Compute the Mahalanobis distances $D_{Mi}(x)$ of the data elements to the center of the data set.

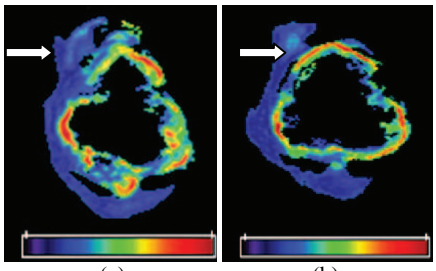
$$D_{Mi}(x) = \sqrt{(X_i - \bar{X}_l)^T \Sigma^{-1} (X_i - \bar{X}_l)}\,, \qquad (7)$$

where Σ is the covariance matrix for each class.
3. Sort $D_{Mi}(x)$ from the smallest to the largest.
4. Select the first half of the sorted data points as the training data set of each tissue type.

Unlike conventional passive learning method (examples are randomly chosen from the training samples), active learning classifier can actively choose the training data and achieve high classification accuracy. In our method, an iterative SVM active learning C-step [12] operation is proposed as the classifier. The C-step operation can generate a subset with smallest determinant of covariance from the previous segmentation results and is used to actively select the training data for each tissue type. After selecting best representing training data in each class, the SVM is trained to segment the entire brain again. Thus, the SVM active learning makes the final segmentation more accurate. List 1 and 2 give the detailed steps of SVM active learning and the C-step operation, respectively.

2.3. Joint Intensity Color-map on Edema Region

Notice that it is not a one-to-one map between the automatic segmentation results and the tumor information. The most important issue is that the non-enhanced tumor has not been label from the results, whereas it is important to highlight the non-enhance tumor to determine the margin of the tumor. Herein, based on the segmentation results, the transition from enhanced tumor region to the normal region is explored using the joint intensity color-maps. First, the mean of the edema class is computed. Then, the Euclidean distance from the multimodal feature of each voxel to that of the edema center is computed. Fig. 3 shows the color-maps for the enhanced and edema areas. Heterogeneity of color-map in the edema (blue) can be observed. This map is informative to neuroradiologists showing potential areas in the edema that likely to be non-enhanced tumor.



(a) (b)

Fig 3. The distance between the features of each voxel and those of the edema centroid.

3. RESULTS

To evaluate our method, we compared its results with those of the knowledge-based fuzzy clustering algorithm and SVM with training sample randomly selected (without the C-step). Manual segmentation was used as the ground truth. Ten samples diagnosed with GBM were used in our experiment. For each subject, the images consist of T2, T1 pre-contrast, T1 post-contrast, and FLAIR scans. The size of the images is $256 \times 256 \times 21$ with voxel size $0.78 \times 0.78 \times 6.5$ mm^3. Fig. 4 shows an example of the segmentation using our method. The subject in Fig. 4 (a) and Fig. 2 is the same, and it can be seen that the edema part has now been classified correctly.

The GBM tissue was manually segmented by an expert to obtain the ground truth. The evaluation of the segmentation performance was carried out by calculating the TPR (true positive rate), and FNR (false negative rate). Suppose A and B represent the sets of pixels segmented

using manual and automatic methods, $TPR = |A \cap B|/|A|$; and $FNR = (|B| - |A \cap B|)/|B|$. Table 1 lists the FPR and FNR for all the ten subjects for different parts of GBM. We can see that our method (a) yields more accurate segmentation results than others.

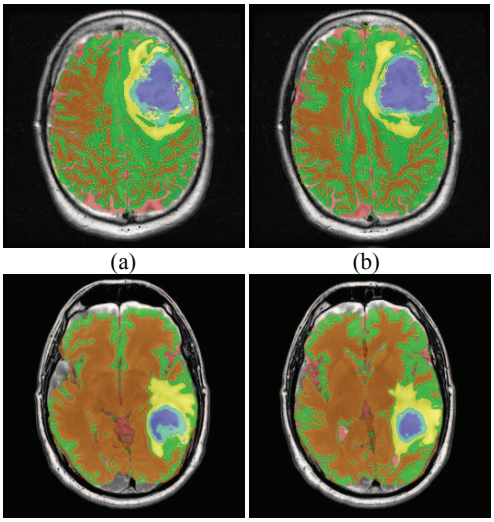


Fig 4. Segmentation results using SVM active learning.

Table 1. Evaluation of segmentation results

(a) SVM active learning

GBM tissue	TPR (average)	FNR (average)
Enhanced Tumor	88.4%	2.8%
Necrosis	86.3%	4.5%
Edema	82.5%	5.1%

(b) Knowledge-based fuzzy clustering method

GBM tissue	TPR (average)	FNR (average)
Enhanced Tumor	77.7%	4.4%
Necrosis	78.4%	9.3%
Edema	74.5%	8.1%

(c) SVM with randomly selected samples

GBM tissue	TPR (average)	FNR (average)
Enhanced Tumor	81.6%	5.3%
Necrosis	79.2%	8.1%
Edema	76.4%	6.8%

4. CONCLUSIONS

We proposed a new SVM active learning approach to GBM segmentation. First, a knowledge-based clustering algorithm was used to obtain the initial segmentation of GBM and generate the training data. Then, the SVM active learning algorithm was performed to optimize the training data set and to refine the segmentation results iteratively. Comparative study showed the proposed method can achieve more accurate results. The color-map showing detailed intensity distributions in edema is currently used as a reference for determining non-enhanced tumor area, but it is lack of quantitative measures. We are calculating the intensity transition from enhanced tumor to edema, and from enhanced tumor to necrosis. Such transition patterns may reflect aggressiveness of GBM. In the future, we plan to conduct a larger scale study to evaluate the robustness of the algorithms for clinical research studies.

5. ACKNOWLEDGEMENT

The authors would like to thank support from NIH grant 5G08LM8937.

6. REFERANCES

[1]. Smirniotopoulos, J.G., The new WHO classification of brain tumors. Neuroimaging Clin N Am, 1999. **9**(4): p. 595-613.

[2]. Van Meir, E.G., et al., Exciting new advances in neuro-oncology: the avenue to a cure for malignant glioma. CA Cancer J Clin, 2010. **60**(3): p. 166-93.

[3]. Verhaak, R.G.W., et al., Integrated genomic analysis identifies clinically relevant subtypes of glioblastoma characterized by abnormalities in PDGFRA, IDH1, EGFR, and NF1. Cancer Cell, 2010. 17(1): p. 98-110.

[4]. Ho, S., E. Bullitt, and G. Gerig, Level Set Evolution with Region Competition: Automatic 3-D Segmentation of Brain Tumors. In ICPR, Quebec, August 2002: p. 532-535.

[5]. Clark, M.C., et al., MRI segmentation using fuzzy clustering techniques. Engineering in Medicine and Biology Magazine, IEEE, 1994. **13**(5): p. 730-742.

[6]. Ozkan, M., B.M. Dawant, and R.J. Maciunas, Neural-Network-Based Segmentation of Multimodal Medical Images - a Comparative and Prospective-Study. IEEE Transactions on Medical Imaging, 1993. **12**(3): p. 534-544.

[7]. Ruan, S., et al., Tumor segmentation from a multispectral MRI images by using support vector machine classification. in ISBI . IEEE, 2007: p. 1236-1239.

[8]. Lee, N., et al., Interactive Segmentation in Multi-Model Imagery using a Bayesian Transductive Learning Approach. SPIE Medical Imaging Conference, 2009.

[9]. Corso, J.J., et al., Efficient multilevel brain tumor segmentation with integrated bayesian model classification. IEEE Trans Med Imaging, 2008. **27**(5): p. 629-40.

[10]. [10]Prastawa, M., et al., A brain tumor segmentation framework based on outlier detection. Med Image Anal, 2004. **8**(3): p. 275-83.

[11]. FSL FLIRT. Available from: www.fmrib.ox.ac.uk/fsl.

[12]. Alexandra Constantin, R. Bajcsy, and S. Nelson, Unsupervised Segmentation of Brain Tissue in Multivariate MRI. In ISBI . IEEE, 2010: p. 89-92.

[13]. Hsu, C.W. and C.J. Lin, A comparison of methods for multiclass support vector machines. IEEE Transactions on Neural Networks, 2002. **13**(2): p. 415-425.

[14]. Pasolli, E., F. Melgani, and Y. Bazi, Support Vector Machine Active Learning Through Significance Space Construction. IEEE Geoscience and Remote Sensing Letters, 2011. **8**(3): p. 431-435.